Decay rates for a class of bistable potentials: Parabolic to wedge-shaped form

H. Risken and Th. Leiber
Abteilung für Theoretische Physik, Universität Ulm, Einsteinallee 11, 7900 Ulm, Federal Republic of Germany
(Received 17 October 1988)

The stochastic relaxation in a class of bistable soft potentials $f(x)=-2\ln[\cosh(x)]+2\ln[\cosh^2(x)+\sinh^2(R)]$ is investigated. The structure of these bistable potentials varies from a smooth parabola to a wedge-shaped behavior as the bistability parameter R increases. It is pointed out that the original (white-noise) Kramers formula for the decay rate applies to such bistable potentials in the *weak-noise limit*, i.e., for small diffusion constants only. An improved analytical prediction for the decay rate valid for small Arrhenius factors is presented. The novel calculation predicts a prefactor that depends on the noise intensity D. This prefactor changes continuously from the Kramers value for small D to the expression for a W-shaped wedge potential for large D. Thus the traditional Kramers theory is extended by this approach. The comparison of our analytical prediction with the numerical results for the smallest nonvanishing eigenvalue is quite convincing for *small Arrhenius factors*. Moreover, a detailed discussion of various mean-first-passage-time (MFPT) and correlation-time expressions in different types of potentials reveals that in the limit of small Arrhenius factors (i) all MFPT's, if applied properly, converge to the smallest nonzero eigenvalue of the corresponding Fokker-Planck equation, and (ii) the structure of the bistable potential at infinity has no dominant influence on the decay rate.

I. INTRODUCTION

In statistical mechanics the diffusion of a Brownian particle in a one-dimensional bistable potential provides a useful model for understanding the stochastic relaxation of an externally driven unstable system towards equilibrium. Since the pioneering work of Kramers,[1] this problem has received much attention because of the important role it plays in many areas of physics and chemistry.[2] Recently renewed interest has been devoted to such systems owing to a special class of potential functions.[3] In Ref. 3 the one-dimensional diffusion in a bistable soft potential was considered, i.e., in a potential with asymptotically constant binding force. The present paper is aimed at pointing out that the conventional Fokker-Planck techniques still apply to bistable soft potentials.

A quantity of major interest in such a bistable system is the mean-first-passage time (T_{MFPT}), that is, the time required for a thermally activated particle to escape from one metastable potential well to a neighboring one.[4-6] In the limit of small Arrhenius factors $\exp(-\Delta f/D)\ll 1$ this MFPT determines the decay rate $\lambda=2/T_{\mathrm{MFPT}}$ of an initial distribution to its stationary state. Throughout this paper we use the equivalent but shorter notation $\Delta f/D\gg 1$, i.e., the noise intensity D is small compared to the barrier height Δf. The decay rate is given by the first nonvanishing eigenvalue of a one-dimensional Fokker-Planck equation (FPE), which describes the process in the overdamped limit. For $\Delta f\gg D$ all higher eigenvalues of the FPE are much larger than $\lambda=\lambda_1$. The analytical methods for obtaining the decay rate in bistable confined (or hard) potentials available in the literature are based, e.g., on the current-over-density or the MFPT approach.[4-7] Only in the limit of large $\Delta f/D$ the connection between the MFPT, the escape rate, and the smallest nonvanishing eigenvalue of the relevant Fokker-Planck operator is well established, see, e.g., Ref. 5. Within this framework the involved integrals are then evaluated in the usual Kramers approximation, which consists of a parabolic expansion of the bistable potential around the well from where the particle escapes and around the top of the potential barrier. Of course higher-order approximations can also be carried out and lead to a reasonable improvement, see Ref. 7 and Sec. IV.

Based on some physical arguments, the MFPT approach has been criticized in Ref. 3 when applied to bistable soft potentials. Various definitions have been proposed in Ref. 3 for substituting the usual MFPT formula of van Kampen.[4] An interesting calculation of the decay rate by means of supersymmetric considerations has also been given in Ref. 3 and the limitations of the usual Kramers formula have already been indicated. However, all calculations given in Ref. 3 have been carried out only for the normalized noise intensity $D=1$.

In the following, it is our aim to present an analytical evaluation of the decay rate for a class of bistable soft potentials with varying shape, which have been investigated in Ref. 3. Our calculation relies on the conventional MFPT expression and is valid for small Arrhenius factors, i.e., $\Delta f/D\gg 1$. In detail we point out, that for the class of bistable soft potentials considered, the weak-noise limit and the limit of small Arrhenius factors, i.e., $\Delta f/D\gg 1$, have to be distinguished. [In the normalization of Eq. (3.1) weak noise means $D\ll 1$.] The difference between these two approaches is explained by a detailed comparison of Kramers's approach and our analytical result for the bistable soft potential. Furthermore, these considerations are corroborated by an expli-

cit investigation of the MFPT problem in bistable confined potentials, i.e., potentials with asymptotically increasing binding forces.

The outline of the paper is the following. In Sec. II we give a brief review of the MFPT problem and its connection with the smallest nonzero eigenvalue of the relevant FPE. The special, bistable, soft potential under study is reported in Sec. III. In Sec. IV we confirm that the parabolic Kramers approximation is valid for bistable soft potentials in the *weak-noise limit* $D \ll 1$ only. An improved (higher-order) Kramers approximation, however, gives better results for the escape rate. Moreover, an analytical formula is presented in Sec. V for the class of soft potentials of Sec. III, which applies for arbitrary noise intensity D provided the barrier height Δf is large enough, i.e., it is valid in the *limit* $\Delta f/D \gg 1$. In particular, for large barrier heights Δf we derive an analytical expression for the prefactor of the Arrhenius law which strongly depends on the noise intensity D and recovers the relevant limits of Kramers's expression for small D and the wedge potential result for large D. All analytical expressions are tested through comparison with the lowest nonvanishing eigenvalue of the Fokker-Planck operator, which is obtained by numerical integration techniques. Finally, a detailed comparison of the conventional MFPT expression,[4] some recent approximations suggested in Ref. 3 and our analytical result are presented in Sec. VI. In Sec. VII we summarize our work.

II. THE FOKKER-PLANCK EQUATION AND THE MEAN FIRST-PASSAGE TIME

The general process under consideration is commonly described by a stochastic differential equation of the Langevin type

$$\dot{x} = -f'(x) + \Gamma(t) , \tag{2.1}$$

where $f(x)$ represents a bistable nonlinear potential (overdot and prime denote differentiation with respect to t and x, respectively) and $\Gamma(t)$ is an external Gaussian white noise of strength D with correlations $\langle \Gamma(t) \rangle = 0$, $\langle \Gamma(t)\Gamma(x) \rangle = 2D\delta(t-s)$. The corresponding FPE is given by

$$\frac{\partial}{\partial t} P(x;t) = \frac{\partial}{\partial x} \left[f'(x) + D\frac{\partial}{\partial x} \right] P(x;t) . \tag{2.2}$$

Following van Kampen,[4] the MFPT from the left minimum $-x_{\min}$ of a symmetric bistable potential to the right minimum $x_{\min}$, denoted by T, reads

$$\begin{aligned} T &= T(-x_{\min}, x_{\min}) , \\ T(x_1, x_2) &= \frac{1}{D} \int_{x_1}^{x_2} \frac{1}{P_{\rm st}(y)} \int_{-\infty}^{y} P_{\rm st}(z)\, dz\, dy , \end{aligned} \tag{2.3}$$

where $P_{\rm st}(x) = \lim_{t \to \infty} P(x;t)$ is the (normalized) stationary solution of the one-dimensional FPE (2.2). $P_{\rm st}(x) = N \exp[-f(x)/D]$ with an appropriate normalization constant N. Equation (2.3) is an exact expression for the MFPT for particles injected at x_1 and absorbed at x_2 with a reflecting wall at $-\infty$. It is valid for arbitrary $\Delta f/D$. For large $\Delta f/D$ one obtains an approximation for twice the inverse of the first nonvanishing eigenvalue describing the transition from the left to the right potential well. The appropriate choice of x_1 and x_2 is then near the left and the right minimum of the bistable potential, respectively; see also the discussion in Ref. 4. (For symmetric potentials one may take x_1 near the left minimum and $x_2 = 0$ thus obtaining an approximation for the inverse of the first eigenvalue.)[8]

For small Arrhenius factors, i.e., $\Delta f/D \gg 1$, the inner integral in (2.3) is almost constant for those y where the integrand of the outer integral has its sharp maximum. Therefore the double integral in (2.3) splits into two single integrals according to

$$T(-x_{\min}, x_{\min}) = \frac{1}{D} I_1 I_2 , \tag{2.4}$$

$$I_1 = \int_{-x_{\min}}^{x_{\min}} \exp[f(x)/D]\, dx ,$$

$$I_2 = \int_{-\infty}^{x_{\max}} \exp[-f(x)/D]\, dx ; \tag{2.5}$$

see also Ref. 7, p. 124. Here $x_{\max}$ denotes the position of the barrier separating the potential wells, and $\pm x_{\min}$ are the positions of the minima of the symmetric potential $f(x)$. In Eq. (2.4) I_2 and $1/I_1$ are proportional to the probability density for finding the Brownian particle in the left potential well and to the probability current over the barrier, respectively.

For small Arrhenius factors, i.e., for $\Delta f/D \gg 1$, the connection between T, the escape rate r from one well, and the smallest nonvanishing eigenvalue λ_1 of the FPE (2.2) (=decay rate λ) is also well established.[5,9] The escape rate for one potential well is given by the reciprocal of the MFPT, while for symmetric potentials the decay rate $\lambda = \lambda_1$ equals twice this escape rate, i.e.,

$$1/T = r = \lambda/2 . \tag{2.6}$$

III. THE BISTABLE SOFT POTENTIAL WITH VARYING SHAPE

We consider the particular potential $f(x)$

$$f(x) = -2 \ln \left[\frac{\cosh(x)}{\cosh^2(x) + \sinh^2(R)} \right] , \tag{3.1}$$

which has been investigated in Ref. 3. The scaling parameters β and γ, which have been used in Ref. 3, can be eliminated by rescaling the time t and the variable x in the FPE (2.2). Therefore we adopt the normalized potential (3.1) in dimensionless units throughout this paper. For the transformed FPE the diffusion D becomes also dimensionless. The potential (3.1) and similar bistable soft potentails arise in the study of the dynamics of sine-Gordon kinks in soliton physics.[10]

In the present case the potential (3.1) exhibits a bistable structure for

$$R > R_0 = \operatorname{arcsinh}(1) = 0.881\,37 \ldots . \tag{3.2}$$

The barrier height is explicitly given by

$$\Delta f = 2\ln\left[\frac{\cosh^2(R)}{2\sinh(R)}\right] \quad \text{for } R \geq R_0$$
$$\approx 2R - 4\ln(2) \quad \text{for } R \gg 1 \; ; \tag{3.3}$$

and thus increases linearly with R for large R. The potential (3.1) exhibits a peculiar structure which is depicted in Figs. 1(a) and 1(b). With increasing bistability parameter R, the regions near the extremal points of the potential become more and more wedge shaped, see Figs. 1(a) and 1(b). [In the limit $R \to \infty$, $f(x)$ recovers the exactly solvable W-shaped wedge potential,[11] if the rescaled variable x/R is used.] A closer inspection of the region near the extremal points in Fig. 1 shows, however, that the deviations from the parabolic expansion occur at the order 1 in the ordinate as well as in the abscissa, almost independent of the bistability parameter R. Details of the potential are only important if they are of the order of or larger than D. Thus for $D \ll 1$, the particle "feels" a parabolic form of the potential near its extrema, whereas for $D \gg 1$ it "feels" a wedge-shaped form. For this reason the parabolic approximation of the potential leading to Kramers's escape rate works well only in the small-noise limit $D \ll 1$. It will be shown that, due to the structure of the potential (3.1) near the extremal points, the usual requirement $\Delta f/D \gg 1$ is not sufficient for the Kramers approximation to hold. This is in contrast to the behavior of the quartic potential (6.15). There, the deviations from the parabolic expansion occur at the order one of the variable x rescaled by the bistability controlling parameter. Obviously, the analytical determination of the MFPT (2.3) involves two levels of approximation, which have to be distinguished. The first one is due to splitting the double integral in Eq. (2.3) while the second approximation step is concerned with the evaluation of the two resulting single integrals (2.5). Our considerations throughout confirm the sensitivity of the second approximation step to the actual potential shape.

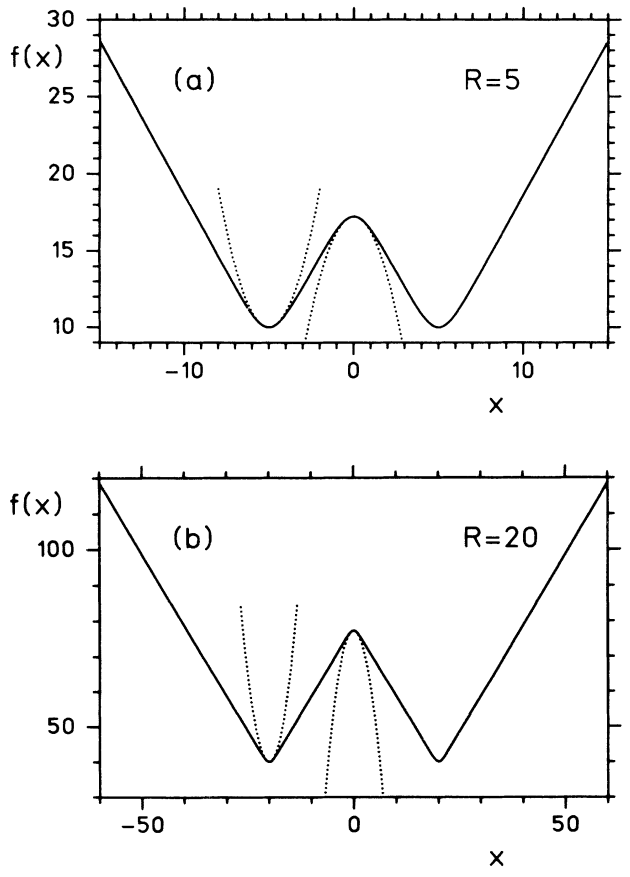

FIG. 1. Bistable soft potential Eq. (3.1) for $R=5$ (a) and $R=20$ (b). The harmonic approximations (dotted line) around the maximum and the left minimum are also shown.

We want to report here some data concerning the special potential (3.1), which we will use later. The positions of the maximum $x_{\max}$ and the minima $\pm x_{\min}$ of the bistable symmetric potential (3.1) are given by

$$x_{\max} = 0, \quad x_{\min} = \operatorname{arccosh}[\sinh(R)]$$
$$\approx R \quad \text{for } R \gg 1 \; . \tag{3.4}$$

With the compact notation $f^{(n)}(x)$ denoting the nth derivative of $f(x)$ with respect to x we have for the potential (3.1)

$$\begin{aligned} f^{(2)}(x_{\max}) &= -2 + 4\cosh^{-2}(R) \; , \\ f^{(3)}(x_{\max}) &= 0 \; , \\ f^{(4)}(x_{\max}) &= 4 + 16\cosh^{-2}(R) - 24\cosh^{-4}(R) \; , \\ f^{(2)}(x_{\min}) &= 2 - 2\sinh^{-2}(R) \; , \\ f^{(3)}(x_{\min}) &= 6[\sinh^2(R) - 1]^{1/2}\sinh^{-3}(R) \; , \\ f^{(4)}(x_{\min}) &= -4 - 8\sinh^{-2}(R) + 18\sinh^{-4}(R) \; . \end{aligned} \tag{3.5}$$

IV. KRAMERS'S ESCAPE RATE IN THE WEAK-NOISE LIMIT $D \ll 1$ (ARBITRARY BARRIER HEIGHT)

In the conventional Kramers approach the integrals I_1 and I_2 in Eq. (2.5) are evaluated in the Gaussian approximation around the relevant potential well and the potential barrier. This parabolic approximation gives the well-known Kramers's escape rate r_K (Refs. 1, 6, and 7),

$$r_K = \frac{1}{2\pi}\sqrt{f''(x_{\min})|f''(x_{\max})|}\exp(-\Delta f/D) \; , \tag{4.1}$$

which has been successfully applied to confined and periodic bistable potentials, see, e.g., Ref. 12. The application of Kramers's formula (4.1) to the potential (3.1) results in the following expression for the decay rate:

$$\begin{aligned} \lambda_K = 2r_K &= \frac{2}{\pi}\frac{\sinh^2(R) - 1}{\cosh(R)\sinh(R)}\exp(-\Delta f/D) \\ &= \frac{2}{\pi}\frac{\sinh^2(R) - 1}{\cosh(R)\sinh(R)}\left[\frac{2\sinh(R)}{\cosh^2(R)}\right]^{(2/D)} \end{aligned} \tag{4.2}$$

This approximation can be improved by employing an expansion of $f(x)$ up to the fourth order, see Ref. 7, p. 124 and also Ref. 13 for a recent application. Using the expli-

cit expressions for the higher-order derivatives of the potential (3.1) reported in Sec. III, we thus obtain the improved Kramers rate

$$\lambda_{\mathrm{IK}}=\lambda_K[1-D\alpha(R)]\ , \tag{4.3}$$

$$\alpha(R)=\tfrac{1}{4}+\tfrac{3}{2}\{\sinh(R)/[\sinh^2(R)-1]\}^2\ . \tag{4.4}$$

For $R\gg1$ the correction factor $\alpha(R)$ becomes $\frac{1}{4}$, i.e.,

$$\lambda_{\mathrm{IK}}=\lambda_K(1-D/4)\quad \text{for } R\gg1\ . \tag{4.5}$$

In Fig. 2 we present the ratios $\lambda_K/\lambda_{\mathrm{num}}$ as a function of D for several bistability parameters R, where λ_{num} denotes the smallest nonvanishing eigenvalue of the FPE (2.2) calculated by means of numerical integration. The integration procedure employed is explained in Sec. 5.9.2 of Ref. 7. One essentially integrates the FPE (2.2) with $(\partial/\partial t)P(x,t)$ replaced by $-\lambda\tilde{P}(x)$ (eigenvalue ansatz). For an odd eigenfunction, the integration procedure starts at $x_{\max}=0$ with the initial conditions $\tilde{P}(0)=0$, and $\tilde{P}'(0)=\text{const}$. The eigenvalue λ is determined by either setting the eigenfunction $\tilde{P}$ or the current $-D\tilde{P}'-f'\tilde{P}$ equal to zero at the upper integration bound $x=x_{\mathrm{end}}$. Physically speaking this corresponds to replacing the potential $f(x)$ for $x=x_{\mathrm{end}}$ by either an absorbing or a reflecting wall. The upper integrational bound should be chosen large enough. In the actual calculation we adopted $x_{\mathrm{end}}=2R+10D$.

From Fig. 2 we immediately recognize that $\lambda_K/\lambda_{\mathrm{num}}$ approaches 1 only for very small D values independent of the bistability parameter R, i.e., no matter what the actual barrier height Δf is. This is due to the special structure of the potential under study. The original Kramers formula (4.1) is applicable to the bistable potential (3.1) only in the small-noise limit $D\ll1$, because the parabolic Kramers approximation of the potential near the extremal points breaks down for larger D values. It is also evident from Fig. 2 that the improved Kramers rate λ_{IK} Eq. (4.3) gives a better approximation for the decay rate which improves with increasing R. In particular, for $R\gtrsim3$, λ_{IK} provides a reasonable approximation for the eigenvalue λ_{num} in the region $0<D\lesssim1$.

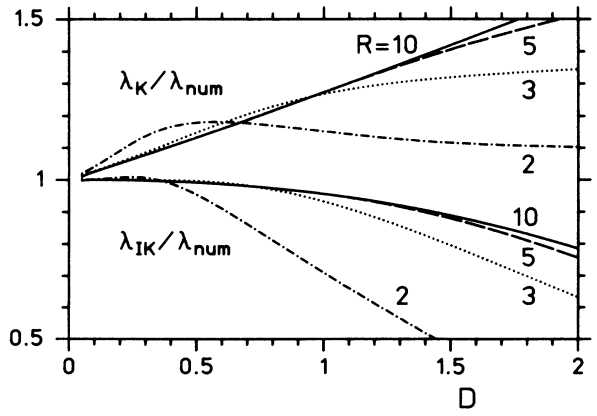

FIG. 2. Ratio of Kramers and improved Kramers approximation λ_K and λ_{IK} and the numerical result λ_{num} as a function of the noise intensity D for different bistability parameters R.

V. DECAY RATE FOR SMALL ARRHENIUS FACTORS (ARBITRARY DIFFUSION)

We continue by evaluating the decay rate for the special bistable soft potential (3.1), which is applicable for arbitrary noise intensity D, provided the barrier separating the two potential wells is high enough, that is in the limit $\Delta f/D\gg1$. In particular, this limit allows for values $D>1$, where the conventional and the improved Kramers rates cannot be applied, see Fig. 2, due to the wedge-shaped structure of the potential (3.1). The basic idea of our approach is to directly evaluate the integrals in Eq. (2.4) in the limit of large R, but without employing any polynomial approximation of the potential $f(x)$. In particular, we thus circumvent the Gaussian approximation, i.e., the parabolic expansion of the potential around its extremal points.

The explicit calculation runs as follows. First we split off the factors $\exp[f(x_{\max})/D]$ and $\exp[-f(x_{\min})/D]$ in the integrals I_1 and I_2 in Eq. (2.5), respectively. According to Eq. (2.6) we replace T by $2/\lambda$ in Eq. (2.4), which is thus transformed to

$$\lambda=\frac{2D}{A_1A_2}\exp(-\Delta f/D)\ , \tag{5.1}$$

$$A_1=\int_{-R}^{R}\left[\frac{\cosh^2(x)+\sinh^2(R)}{\cosh(x)\cosh^2(R)}\right]^{(2/D)}dx\ , \tag{5.2a}$$

$$A_2=\int_{-\infty}^{0}\left[\frac{2\sinh(R)\cosh(x)}{\cosh^2(x)+\sinh^2(R)}\right]^{(2/D)}dx\ . \tag{5.2b}$$

For large values of R the integrand of Eq. (5.2a) can be safely replaced by $[\cosh(x)]^{(-2/D)}$. Then the integration limits of the integral A_1 are replaced by $\pm\infty$. On the other hand, the integrand of Eq. (5.2b) has a distinct maximum around $x\approx-R$. Therefore it is approximated in the limit $R\gg1$ near $x=-x_{\min}\approx-R$ by

$$\frac{2\sinh(R)\cosh(x)}{\cosh^2(x)+\sinh^2(R)}\approx2\frac{e^Re^{-x}}{e^{-2x}+e^{2R}}=\frac{1}{\cosh(x+R)}\ . \tag{5.3}$$

Now a simple variable substituion $x+R\rightarrow x$ is employed. Replacing the new upper boundary R of the transformed integral (5.2b) with ∞ we finally obtain

$$A_1=A_2=\int_{-\infty}^{\infty}[\cosh(x)]^{(-2/D)}dx\ . \tag{5.4}$$

The integration of Eq. (5.4) (see formula 3.512 of Ref. 14) and the application of formula 8.384.1 and the doubling formula 8.335.1 of Ref. 14 for the Γ function gives

$$A_1=A_2=\sqrt{\pi}\frac{\Gamma(1/D)}{\Gamma(1/2+1/D)}\ . \tag{5.5}$$

The insertion of Eq. (5.5) into Eq. (5.1) thus yields the special result for the decay rate

$$\lambda_S=\Omega(D)\exp(-\Delta f/D)\ , \tag{5.6}$$

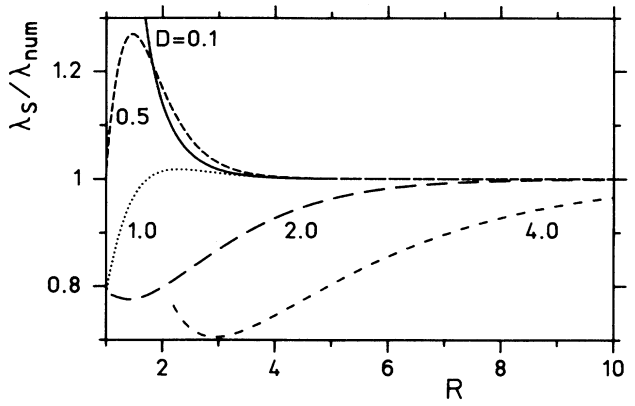

FIG. 3. Ratio of the special result λ_S and the numerical result λ_{num} as a function of the bistability parameter R for different noise intensities D.

$$\Omega(D)=\frac{2D}{\pi}\left[\frac{\Gamma(1/2+1/D)}{\Gamma(1/D)}\right]^2 . \tag{5.7}$$

The ratio of λ_S and the numerical value λ_{num} as a function of the bistability parameter R is shown in Fig. 3. Clearly, the analytical approximation λ_S for the small eigenvalue applies for a wide range of D values, provided R is large enough. (Note that the evaluation of λ_S relies on the assumption $R \gg 1$.) For $D > 1$ and decreasing R the lowest nonzero discrete eigenvalue λ_{num} reaches the lower bound $\lambda_{cont}=1/D$ of the continuous part of the spectrum at a certain value $R_{crit} \geq R_0$. Therefore λ_{num} does not exist for $R < R_{crit}$.

Discussion of the prefactor $\Omega(D)$

It is interesting to note that the prefactor $\Omega(D)$ depends on the noise intensity D. For the sake of completeness we report here some special values of Ω

$$\Omega(0.5)=\tfrac{9}{16},\quad \Omega(1)=\tfrac{1}{2},\quad \Omega(2)=4/\pi^2 . \tag{5.8}$$

Next we discuss the asymptotic behavior of the prefactor. For small values of the noise intensity D, we use Stirling's formula for the Γ function and obtain for the prefactor

$$\Omega(D)=\frac{2}{\pi}(1-D/4)+O(D^2) , \tag{5.9}$$

and thus recover the improved Kramers result (4.5) valid for large R. For large D we employ a Taylor expansion of $\Gamma(1/2+1/D)$ and of $\Gamma(1+1/D)=\Gamma(1/D)/D$ and get

$$\Omega(D)=\frac{2}{D}\left[1-\frac{4\ln(2)}{D}\right]+O(D^{-3}) . \tag{5.10}$$

In the large-D limit the special result λ_S Eq. (5.6) with the leading term $2/D$ of the prefactor in Eq. (5.10) is just the lowest nonzero eigenvalue of the (W-shaped) wedge potential

$$\begin{aligned} f(x)&=2R(1-|x|/R), \quad |x|<R , \\ f(x)&=2R(|x|/R-1), \quad |x|>R , \end{aligned} \tag{5.11}$$

which has been investigated by Mörsch *et al.*, see Ref. 11, Eq. (57). [For an explicit comparison the variable transformation of Eq. (3) in Ref. 11 has to be considered.]

From the asymptotic expressions (5.9) and (5.10) one can derive a [1/2]-Padé approximation Ω_P for the prefactor of the decay rate (see Ref. 15 for details on Padé approximations),

$$\Omega_P=\frac{2}{\pi}\frac{1+aD}{1+(a+\frac{1}{4})D+D^2a/\pi} , \tag{5.12}$$

$$\begin{aligned} a&=\{\pi-1+[(\pi-1)^2+4\pi\ln(2)]^{1/2}\}/[8\ln(2)] , \\ &=1.0438\ldots . \end{aligned} \tag{5.13}$$

In Fig. 4 the prefactors of the decay rates from the various analytical predictions are shown. The solid line and the dotted line represent the exact expression (5.7) and the corresponding Padé approximant (5.12), respectively. The Padé approximation (5.12) has been derived by fitting the asymptotic expressions (5.9) and (5.10). The small deviation of the Padé approximation (5.12) from the exact expression (5.7) for intermediate D values is hardly visible in Fig. 4. (An alternative [1/2]-Padé approximation, which reproduces the asymptotic expression (5.9) and recovers the first-order term in Eq. (5.10) and the exact value 0.5 for $D=1$, leads to $a=(16-5\pi)/(4\pi-12)$ $=0.5156\ldots$.)

Obviously, Fig. 4 summarizes our results of Secs. IV and V for large R, i.e., $R \gtrsim 3$. The Kramers rate may be safely applied to the bistable potential under study in the region $D \lesssim 0.1$. The higher-order approximation of the potential near the extremal points adopted in the improved Kramers approximation extends the range of applicability to $D \lesssim 1$. On the other hand, for $D \gtrsim 40$ potential (3.1) can be safely replaced by the W potential, which has been investigated in Ref. 11. In the intermediate

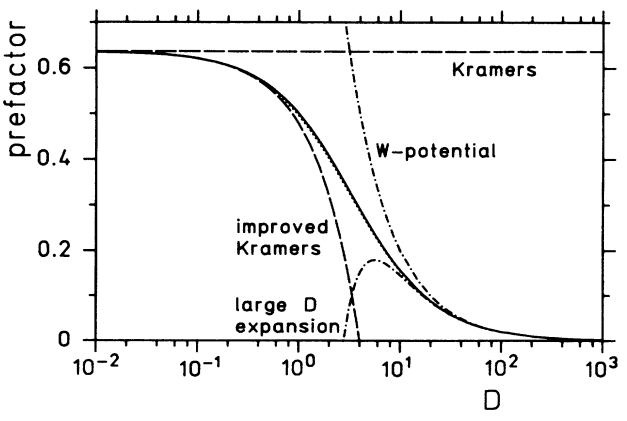

FIG. 4. The prefactor $\Omega(D)$ and its approximations as a function of the diffusion constant D. The solid line gives the exact expression for $\Omega(D)$, Eq. (5.7), and the dotted line is the Padé approximation $\Omega_P(D)$, Eq. (5.12). The other approximations are indicated in the figure.

range $1 \lesssim D \lesssim 40$, however, either the exact formula (5.7) for the prefactor or its Padé approximant (5.12) must be used.

Finally we want to compare the special result λ_S and the improved Kramers result $\lambda_{\rm IK}$ with the relevant eigenvalue calculated in Ref. 3 by exploiting the property of isospectrality of supersymmetric quantum mechanics. Only the case $D=1$ was treated in that reference. Therefore we have to restrict the comparison to this value. For $D=1$ and $R \gg 1$ Eqs. (5.6) and (3.3) give

$$\lambda_S = 8\exp(-2R)\ , \tag{5.14}$$

which coincides exactly with the analytic result derived by Marchesoni *et al.*[3] The integral expression (5) of Ref. 3 coincides very well with our $\lambda_{\rm num}$. The maximum deviation is about 0.06% for $R \approx 2$. We note that the improved Kramers approximation (4.3) already leads to a value reasonably close to Eq. (5.14), i.e.,

$$\lambda_{\rm IK} = \frac{3}{\pi} 8\exp(-2R) = (7.639\ldots)\exp(-2R)\ , \tag{5.15}$$

whereas the original Kramers result

$$\lambda_K = \frac{4}{\pi} 8\exp(-2R) = (10.185\ldots)\exp(-2R) \tag{5.16}$$

yields a rather poor quantitative agreement as already mentioned in Ref. 3.

VI. VARIOUS MFPT EXPRESSIONS IN COMPARISON WITH THE DECAY RATE

In this section we give a detailed comparison between various analytical MFPT and decay-rate expressions and the lowest nonvanishing eigenvalue of the FPE (2.2) obtained numerically. For the sake of completeness this comparison is carried out for the bistable soft potential (3.1) and for an archetypal bistable hard potential.

First we report some analytical expressions for the decay rate λ given in Refs. 3 and 4:

$$\lambda_a \equiv 2/T(-x_{\rm min}, x_{\rm min})\ , \tag{6.1}$$

$$\lambda_b \equiv 1/T(-x_{\rm min}, 0)\ , \tag{6.2}$$

$$\lambda_c \equiv 1/\langle T(x_1,0)\rangle_{x_1<0} = \frac{2}{D}\int_{-\infty}^{0}\left[\int_{-\infty}^{x} P_{\rm st}(y)dy\right]^2 \frac{1}{P_{\rm st}(x)}dx\ , \tag{6.3}$$

$$\lambda_d \equiv 1/T_c = \frac{2}{D\langle x^2\rangle}\int_{-\infty}^{0}\left[\int_{-\infty}^{x} yP_{\rm st}(y)dy\right]^2 \frac{1}{P_{\rm st}(x)}dx\ , \tag{6.4}$$

$$\langle x^2\rangle = \int_{-\infty}^{\infty} x^2 P_{\rm st}(x)dx\ .$$

Here Eqs. (6.1) and (6.2) rely on van Kampen's formula (2.3). Thus, in accordance with Eq. (6.5) of Ref. 4, we ask for the mean time a particle needs to reach the right minimum $x_{\rm min}$, or the potential barrier $x=0$ in Eqs. (6.1) and (6.2), respectively, if the particle had been injected at the left minimum $-x_{\rm min}$. By manipulating the integrals in the definitions (6.1) and (6.2), it can be shown that for symmetric potentials $[f(x)=f(-x) \rightarrow P_{\rm st}(x)=P_{\rm st}(-x)]$ the following relation holds:

$$\frac{1}{\lambda_a} - \frac{1}{\lambda_b} = \int_0^{x_{\rm min}} \frac{dx}{P_{\rm st}(x)} \int_0^x P_{\rm st}(y)dy > 0\ . \tag{6.5}$$

Thus λ_a is always less than λ_b. This can also be interpreted physically. Namely, if the particles injected at $-x_{\rm min}$ reach the top of the barrier at $x=0$, they have a 50% chance to go back to the left well or to move to the right well. Therefore $T(-x_{\rm min}, x_{\rm min})$ is at least twice as large as $T(-x_{\rm min}, 0)$. If the particles have crossed the top of the barrier they still need some additional time ΔT to reach the bottom of the right well. Thus we have

$$T(-x_{\rm min}, x_{\rm min}) = 2T(-x_{\rm min}, 0) + \Delta T\ , \qquad \Delta T = 2\left[\frac{1}{\lambda_a} - \frac{1}{\lambda_b}\right]\ . \tag{6.5a}$$

The difference ΔT is much smaller than $2T(-x_{\rm min}, 0)$ for large barrier heights, and therefore λ_a and λ_b become almost identical.

On the other hand, Eqs. (6.3) and (6.4) have been claimed in Ref. 3 to supply a more refined approximation for the lowest nonvanishing eigenvalue in the bistable soft potential (3.1). According to Eq. (6.3) $1/\lambda_c$ is obtained on averaging $T(x_1, x_2=0)$ [see Eq. (2.3)] with respect to the normalized distribution function $2P_{\rm st}(x_1<0)$ of the negative starting points.[3] In other words, the particles are injected at any negative x_1 and the starting points are weighted according to the stationary distribution function. We are then interested in the mean time it takes the particles to reach the potential barrier at $x=0$. Finally, Eq. (6.4) is an attempt to substitute $1/\lambda$ with the autocorrelation time of the variable $x(t)$, see Ref. 3, Eq. (10). The definition (6.3) can also be interpreted in terms of correlation times. This can be seen as follows. The correlation time T of a general autocorrelation function

$$K_r(\tau) = \langle [r(x(t)) - \langle r\rangle][r(x(t+\tau)) - \langle r\rangle]\rangle\ , \qquad \langle r\rangle = \int r(x)P_{\rm st}(x)dx \tag{6.6}$$

may be defined by the integral over the normalized correlation function $K_r(\tau)/K_r(0)$

$$T = \int_0^{\infty} K_r(\tau)d\tau / K_r(0)\ . \tag{6.7}$$

It has been shown in Ref. 16 that the correlation time T in one-dimensional stochastic systems can be expressed by integrals, e.g.,

$$T = \frac{1}{K_r(0)}\frac{1}{D}\int_{-\infty}^{\infty}\frac{1}{P_{\rm st}(x)}\left[\int_{-\infty}^{x}[r(x') - \langle r\rangle] \times P_{\rm st}(x')dx'\right]^2 dx\ . \tag{6.8}$$

Equation (6.8) represents a generalization of Eq. (2.43) of Ref. 16, because it describes the correlation time of an arbitrary function $r(x)$ of the variables $x(t)$, instead of $x(t)$ itself. (Of course, we assume that the integrals exist.)

Since in our actual problem the variable $x(t)$ extends to $-\infty$, the lower integration bound in Eq. (2.43) of Ref. 16 has to be replaced by $-\infty$. The function $g^2(x)$ in Eq. (2.43) of Ref. 16 is identified with the diffusion constant D (additive noise). For symmetric potentials $f(x)=f(-x)$ and odd functions $r(x)=-r(-x)$, the mean value $\langle r \rangle$ in Eq. (6.8) vanishes. Hence the integrand of the first integral in Eq. (6.8) is an even function, and we replace Eq. (6.8) with twice the integral over the half range of x,

$$T=\frac{2}{K_r(0)}\frac{1}{D}\int_{-\infty}^{0}\frac{1}{P_{\rm st}(x)}\left[\int_{-\infty}^{x} r(x')P_{\rm st}(x')dx'\right]^2 dx \ . \tag{6.8a}$$

Obviously, for $r(x)=x$, Eq. (6.8a) recovers exactly T_c of Eq. (6.4). If $r(x)$ in Eq. (6.8a) denotes the step function

$$r(x)\equiv\Theta(x)-\Theta(-x)=\begin{cases}1 & \text{for } x>0\\ -1 & \text{for } x<0\end{cases} \tag{6.9}$$

[$\Theta(x)$ is the Heaviside stepfunction], it is evident that Eq. (6.8a) reproduces $\langle T(x_1,0)\rangle_{x_1<0}$ of Eq. (6.3).

It follows from the expansion of the Green's function of the FPE with a discrete eigenvalue spectrum [see, e.g., Eq. (5.46) of Ref. 7], that for symmetric potentials the inverse correlation time of any autocorrelation function of an odd function $r(x)$ is always larger than or equal to the lowest nonvanishing eigenvalue. This property is preserved if the eigenvalue spectrum has a continuous part. [For R larger than the critical value $R_{\rm crit}$ the spectrum consists at least of two discrete eigenvalues, 0 and λ_1, and a continuum $\lambda \geq 1/D$; see the discussion below Eq. (5.7) and Sec. VII.] Thus λ_c and λ_d provide upper bounds for the eigenvalue λ_1, i.e.,

$$\lambda_c,\lambda_d \geq \lambda_1=\lambda \ . \tag{6.10}$$

The asymptotic behavior of λ_{b-d} can be evaluated similarly as in Sec. V, and it turns out that the asymptotic values for λ_{a-c} coincide, i.e.,

$$\lambda_a=\lambda_b=\lambda_c=\lambda_S \quad \text{for } \Delta f/D \gg 1 \ . \tag{6.11}$$

The favorite proposal of Ref. 3, however, exhibits a different asymptotic behavior

$$\lambda_d=\lambda_{AS}=\lambda_S[1+\mu(D)/R^2] \quad \text{for } \Delta f/D \gg 1 \tag{6.12}$$

with $\mu(D)$ given by

$$\mu(D)=\left[\int_0^\infty x^2[\cosh(x)]^{(-2/D)}dx\right]\Big/\left[\int_0^\infty[\cosh(x)]^{(-2/D)}dx\right] \ . \tag{6.13}$$

For $D=1,2$ Eq. (6.13) yields

$$\mu(1)=\pi^2/12, \quad \mu(2)=\pi^2/4 \ . \tag{6.14}$$

In Fig. 5 we show the expressions λ_{a-d} and the approximations λ_K, $\lambda_{\rm IK}$, and λ_S divided by the lowest nonvanishing eigenvalue $\lambda_{\rm num}$, determined numerically, as a function of $\Delta f/D$. Let us briefly summarize the main points that should be recognized from Fig. 5.

(i) For small potential barriers $\Delta f/D \lesssim 2$ the analytical predictions λ_{a-d} describe different physical situations. [In this regime the MFPT depends strongly, e.g., on the integration bounds x_1 and x_2 of Eq. (2.3).] Therefore deviations from the numerically exact eigenvalue occur in this region.

(ii) At the end of the bistability region $\Delta f/D \to 0$, λ_a and λ_b diverge, because $x_{\rm min}$ tends to zero for $\Delta f \to 0$.

(iii) The expressions λ_{a-c} converge to $\lambda_{\rm num}$ very fast in the limit $\Delta f/D \gg 1$. The relative error seems to be of the order of the Arrhenius factor $\exp(-\Delta f/D)$.

(iv) The expression λ_d approximates the eigenvalue reasonably close near $\Delta f/D \approx 0$ and fairly well in the whole bistability region, but it converges much more slowly to $\lambda_{\rm num}$ than λ_{a-c} for large $\Delta f/D$. It converges, however, very fast to its asymptotic form (6.12). The good agreement between λ_d and $\lambda_{\rm num}$ near the end of the bistability region at $\Delta f/D=0$ is related to the fact that the (almost) monostable potential can be well approximated by a parabola (structural details of the potential which are smaller than D are unimportant). For a parabolic potential, however, the correlation time of the autocorrelation function $K_x(t)$ is exactly equal to the inverse of the first nonvanishing eigenvalue.

(v) As discussed before $\lambda_{\rm IK}$ turns out to supply a reasonable improvement over λ_K; both, however, converge to a value different from $\lambda_{\rm num}$ for $\Delta f/D \gg 1$.

(vi) Our analytical approximation λ_S reproduces the eigenvalue $\lambda_{\rm num}$ very well for $\Delta f/D \gg 1$, and the relative error is also of the order of the Arrhenius factor. Finally, we note that our analytical approximation λ_S of λ_a is in better agreement with $\lambda_{\rm num}$ than λ_a itself for $\Delta f/D \gtrsim 0.3$. This is just an artifact of the approximation

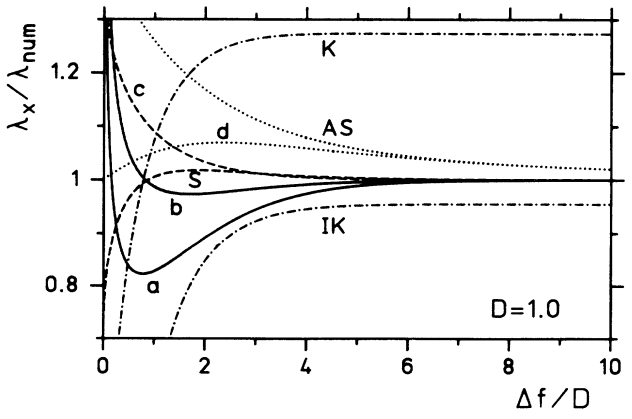

FIG. 5. Various ratios $\lambda_x/\lambda_{\rm num}$ for the bistable *soft* potential (3.1) as a function of the ratio $\Delta f/D$ for $D=1$. The barrier height Δf is given by Eq. (3.3). The index x in λ_x stands for $a-d$, see Eqs. (6.1)–(6.4); K, see Eq. (4.2); IK, see Eq. (4.3); S, see Eq. (5.6); and AS, see Eq. (6.12).

carried out in Sec. V and due to our choice of $D=1$. Similar investigations for $D=0.5,2.0$ show that the behavior of λ_S changes considerably with the noise intensity D for small values of $\Delta f/D$.

For the sake of comparison we have also investigated the quartic double-well (hard) potential

$$f_Q(x)=-ax^2/2+x^4/4 . \tag{6.15}$$

The barrier height is given by

$$\Delta f_Q=a^2/4, \quad a>0 . \tag{6.16}$$

The explicit results are shown in Fig. 6. An inspection of Figs. 5 and 6 confirms that there exists no qualitative difference between the bistable soft potential (3.1) and the bistable hard potential (6.15) with respect to the MFPT problem. The only principal difference is due to the structure of the potentials near the extremal points. The quartic potential (6.15) is well approximated by a parabola near the extremal points in an increasing interval of x values as the barrier height increases. This is not the case for the class of bistable soft potentials (3.1) as pointed out before. Therefore, the Kramers rate and especially the improved Kramers rate work very well in the quartic potential (6.15) for large $\Delta f/D$ even for arbitrary $D>0$.

Finally we comment on a simple, bistable model potential. The eigenvalue λ_1 (as well as all the other eigenvalues) and the expressions λ_{a-d} can be calculated analytically for arbitrary barrier heights in a bistable square well potential, see, e.g., Ref. 7, Sec. 5.7 or Ref. 11. The results are essentially the same as for the bistable soft potential and the quartic double well potential in Figs. 5 and 6, respectively. The most important difference are the following.

(i) The expressions λ_a and λ_b do not diverge for $\Delta f\to 0$, because $x_{\min}$ (defined as the middle of the square well) does not tend to zero in this limit.

(ii) For large $\Delta f/D$ the ratio $(\lambda_d-\lambda_{\text{num}})/\lambda_{\text{num}}$ converges to a finite value, which is given by $\frac{1}{27}$.

(iii) Of course, the Kramers approximations do not exist in the square-well potential.

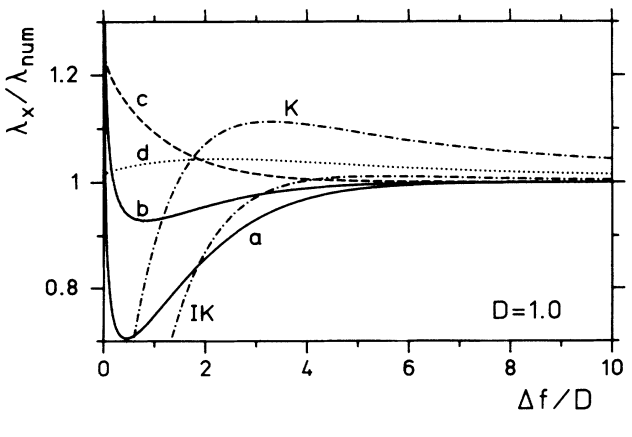

FIG. 6. Same as Fig. 5 but for the (quartic) bistable *hard* potential (6.15) for $D=1$. The barrier height Δf is given by Eq. (6.16). The analytic results λ_S and λ_{AS} do not exist in this case.

VII. SUMMARY AND DISCUSSION

We have pointed out the limitations of applicability of the conventional Kramers formula (4.1) for a potential where the usual parabolic approximation for arbitrary noise intensity D is not possible. An improved Kramers formula (4.3) taking into account higher-order derivatives of the potential gives somewhat better results in the weak-noise limit. The comparison of the special result λ_S, however, is quite favorable for arbitrary D in the limit $\Delta f/D\gg 1$.

The proposed procedure for calculating λ_S is valid within the conventional current-over-density approach and may also find application for different types of potentials which resist the parabolic Kramers approximation. Thus, contrary to what is stated in Ref. 3, the conventional Fokker-Planck techniques also apply to the bistable potential (3.1). The limitations of applicability of the different approaches are not due to the softness of the potential under study but arise because of its shape near the extremal points. In the limit $\Delta f/D\gg 1$ the usual current-over-density approach for the MFPT problem works well.

With another argument we also conclude that the softness of the potential does not cause troubles in the limit of small Arrhenius factors. It follows by inspection of the corresponding Schrödinger potential

$$V_S(x)=f'^2(x)/(4D)-f''(x)/2$$

that $f'(x)$ is a constant for large values of $|x|$, and therefore V_S is also constant, $V_S=1/D$. The lower bound of the continuous part of the eigenvalue spectrum is thus given by $\lambda_{\text{cont}}=1/D$. For $\Delta f/D\gg 1$ the smallest nonvanishing (discrete) eigenvalue, i.e., the decay rate λ, is proportional to the Arrhenius factor $\exp(-\Delta f/D)$. Since the Arrhenius factor is much smaller than the continuum bound $\lambda_{\text{cont}}=1/D$ the computed lowest eigenvalue always corresponds to a bounded eigenfunction which decreases exponentially with increasing $|x|$.

A detailed investigation of the numerical result λ_{num} with respect to the different boundary conditions employed in the numerical integration procedure clarifies the discussion even more. In general, if we set the current equal to zero at $x=\pm x_{\text{end}}$ (reflecting wall=hard potential) the corresponding eigenvalue λ_{num} is smaller than the eigenvalue computed from the absorbing wall boundary condition, $\tilde{P}=0$ at $x=\pm x_{\text{end}}$. However, if x_{end} is taken large enough both eigenvalues agree within the prescribed numerical accuracy. In other words, in the limit $\Delta f/D\gg 1$ the localized eigenfunction corresponding to the smallest nonvanishing eigenvalue is practically independent of the shape of the potential at very large x.

Finally we want to emphasize that the analytic expressions for the decay rate, which have been discussed in Secs. V and VI, are exactly valid only in the limit $\Delta f/D\to\infty$. For large but finite $\Delta f/D$ the relative error is of the order of the Arrhenius factor $\exp(-\Delta f/D)$ for not too small D. Thus, e.g., for $\Delta f/D=5$ the relative error is of the order 1%, see Fig. 5. For small and intermediate $\Delta f/D$ we do not know an analytic expression for the lowest nonvanishing eigenvalue (decay rate). In this

regime van Kampen's formula (2.3) (or similar definitions) may be used for calculating the MFPT. Due to the different integration boundaries, which describe different physical situations, the MFPT's are generally not equivalent. The decay of initial distributions to the stationary state is also more complicated in this regime, because the actual description now involves contributions from the continuous part of the eigenvalue spectrum. Obviously the connection (2.6) between the MFPT and the smallest nonvanishing (discrete) eigenvalue λ_1 breaks down for small and intermediate $\Delta f/D$.

ACKNOWLEDGMENTS

We wish to thank Dr. F. Marchesoni for stimulating discussions and Professor F. Moss and Dr. H. D. Vollmer for reading and improving the manuscript. Financial support from the Deutsche Forschungsgemeinschaft is also gratefully acknowledged.

[1]H. A. Kramers, Physica **7**, 284 (1940).

[2]T. Fonseca, J. A. N. F. Gomes, P. Grigolini, and F. Marchesoni, Adv. Chem. Phys. **62**, 389 (1985); R. Cristiano and P. Silvestrini, J. Appl. Phys. **60**, 3243 (1986); D. Chandler, J. Stat. Phys. **42**, 49 (1986); G. R. Fleming, S. H. Courtney, and M. W. Balk, J. Stat. Phys. **42**, 83 (1986); J. T. Hynes, *ibid.* **42**, 149 (1986).

[3]F. Marchesoni, P. Sodano, and M. Zannetti, Phys. Rev. Lett. **61**, 1143 (1988).

[4]N. G. van Kampen, *Stochastic Processes in Physics and Chemistry* (North-Holland, Amsterdam, 1981), p. 328.

[5]P. Talkner, Z. Phys. B **68**, 201 (1987).

[6]K. Schulten, Z. Schulten, and A. Szabo, J. Chem. Phys. **74**, 4426 (1981); for a recent review see P. Hänggi, J. Stat. Phys. **42**, 105 (1986).

[7]H. Risken, *The Fokker-Planck Equation* (Springer-Verlag, Berlin, 1984).

[8]In Ref. 3 the limit $x_1 \to -\infty$ was considered. This means that the particles are injected at $x = -\infty$. In order to reach the right well the particles need an infinitely long time to travel this infinite distance. [Because the potential is linear for large negative values of x (constant force), overdamped particles cannot gain infinite velocities.] Thus $T(x_1,0)$ diverges for $x_1 \to -\infty$. In this limit the expression $T(-\infty,0)$ cannot be compared with the inverse of the first nonvanishing eigenvalue describing the transition from the left to the right well.

[9]P. Jung and P. Hänggi, Phys. Rev. Lett. **61**, 11 (1988).

[10]S. de Lillo and P. Sodano, Lett. Nuovo Cimento **37**, 380 (1983); P. Sodano, C. R. Willis, and M. El-Batanouny, Phys. Rev. B **34**, 4936 (1986); O. Hudak and L. Trlifaj, J. Phys. A **18**, 445 (1985); D. K. Campbell, M. Peyrard, and P. Sodano, Physica **19D**, 165 (1986).

[11]M. Mörsch, H. Risken, and H. D. Vollmer, Z. Phys. B **32**, 245 (1979).

[12]P. Jung and H. Risken, Z. Phys. B **61**, 367 (1985); Th. Leiber, F. Marchesoni, and H. Risken, Phys. Rev. A **38**, 983 (1988).

[13]Th. Leiber and H. Risken, Phys. Rev. A **38**, 3789 (1988).

[14]I. S. Gradsteyn and I. M. Ryzhik, *Tables of Integral Series and Products* (Academic, New York, 1965).

[15]G. A. Baker, Jr., *Essentials of Padé Approximants* (Academic, New York, 1975).

[16]P. Jung and H. Risken, Z. Phys. B **59**, 469 (1985).